Electric fields in ice and near water clusters

Enrique R. Batista
*Department of Physics, P.O. Box 351560, University of Washington, Seattle, Washington 98195-1560
and Department of Chemistry, P.O. Box 351700, University of Washington, Seattle,
Washington 98195-1700*

Sotiris S. Xantheas[a]
*Environmental Molecular Sciences Laboratory, Pacific Northwest National Laboratory,
906 Battelle Boulevard, P.O. Box 999, MS K8-91, Richland, Washington 99352*

Hannes Jónsson[b]
Department of Chemistry, P.O. Box 351700, University of Washington, Seattle, Washington 98195-1700

We have studied the electric field near water clusters and in ice Ih using first principles calculations. We employed Møller–Plesset perturbation theory (MP2) for the calculations of the clusters up to and including the hexamer, and density functional theory (DFT) with a gradient dependent functional [Perdew–Wang (PW91)] for ice Ih as well as the clusters. The electric field obtained from the first principles calculations was used to test the predictions of an induction model based on single center multipole moments and polarizabilities of an isolated water molecule. We found that the fields obtained from the induction model agree well with the first principles results when the multipole expansion is carried out up to and including the hexadecapole moment, and when polarizable dipole and quadrupole moments are included. This implies that accurate empirical water interaction potential functions transferable to various environments such as water clusters and ice surfaces could be based on a single center multipole expansion carried out up to the hexadecapole. Since point charges are not included, the computationally intensive Ewald summations can be avoided. Molecular multipole moments were also extracted from the first principles charge density using zero flux dividing surfaces as proposed by Bader. Although the values of the various molecular multipoles obtained with this method are quite different from the ones resulting from the induction model, the rate of convergence of the electric field is, nevertheless, quite similar. © *2000 American Institute of Physics.* [S0021-9606(00)52505-7]

I. INTRODUCTION

The interaction between water molecules, including arrangements that exhibit hydrogen bonding, is believed to be largely electrostatic and is typically modeled simply by placing point charges on or near the O and the H atoms in each water molecule. Such models are typically tailored to be consistent with various properties of liquid water, but may not reproduce accurately the electric fields in other environments, such as water clusters, ice, surfaces, and interfaces. The more sophisticated point charge models also include polarizable point dipoles which greatly improve their ability to reproduce diverse environments.[1–4] A frequently discussed quantity is the dipole moment of water molecules in various environments, such as clusters and condensed phases (see, for example, Refs. 3,5–18). The dipole moment of a water molecule in ice and in the liquid is estimated to be significantly larger than the dipole moment of an isolated water molecule[5,16–18] as a result of the polarization of the individual water molecules from their neighbors.

A systematic approach to modeling the electric field around water molecules is the induction model, where a multipole expansion of the electron density is carried out.[5,19–21]

The effect of external field on the multipoles is included through the molecular polarizability. The most straightforward approach is to expand the electron density about one center on each molecule, for example the center-of-mass. It is not clear, however, what order in the multipole expansion is required to accurately represent the electric field at distances relevant to molecular interactions, and whether polarizabilities of isolated molecules can be used for water molecules in condensed phases, such as ice. More sophisticated multipole expansions have been used by Stone, Buckingham, and co-workers [20,21] where several multipole expansion centers are included on each molecule, the so called distributed multipole approach. The expansion then typically includes point charge terms even for neutral molecules such as water.

First principle calculations nowadays can be carried out at a level that is sufficient to accurately reproduce the interaction between water molecules. Such calculations can provide important information about the electric field and can be used to test various empirical or semiempirical descriptions of the interactions. The first principles calculations can also be used as a means to extract molecular multipoles. Several first principles studies have reported values for the molecular dipole moment of water in various environments.[9–14,17,18] The partition of either the wave function or the electronic charge density among the individual molecules in a system of two or more molecules is not, however, unique. Several

a)Electronic mail: sotiris.xantheas@pnl.gov
b)Electronic mail: hannes@u.washington.edu

schemes for achieving this goal have been previously proposed[22–28] invoking different criteria for assigning pieces of the electron density or the wave function to individual molecules. Nevertheless, different partition schemes can lead to widely different values for the multipole moments.[29]

We report here on studies of the electric field in water clusters and ice Ih based on first principles calculations. We compare the electric field obtained from the first principles calculations with electric fields predicted by a simple induction model based on a multipole expansion around the center-of-mass of the molecules. This establishes the order in the multipole expansion that is required to reproduce the electric field obtained from first principles and tests whether the use of gas phase molecular polarizabilities is appropriate in order to model condensed phase environments. It has been previously shown that for clusters of diatomic molecules, such as HF and CO, it is sufficient to include up to quadrupole terms,[30] but H_2O is likely to require higher multipoles. Self-consistent field (SCF) calculations of polarizabilities of urea dimer and trimer have suggested that additivity of molecular polarizabilities can be a good approximation for small clusters.[31] Changes in the polarizability due to slight changes in the molecular geometry have also been found to be small.[32–34] These earlier studies support the notion that an induction model may indeed be a good approximation for describing molecular interactions. In this study we carry out rigorous tests of this proposition for water clusters by investigating how accurately the induction model reproduces the electric field obtained from first principles calculations.

We have also used the results of first principles calculations to extract molecular multipole moments and compare those with values obtained from the induction model. In Sec. II we outline the technical details of the first principles calculations. For completeness, the induction model is described in Sec. III. Our results are presented in Sec. IV and are discussed further in Sec. V.

II. FIRST PRINCIPLES CALCULATIONS

Our goal is to assess the ability of the induction model to reproduce the electric field for ice Ih by comparing its results with the ones obtained from first principles calculations for this system. The need to perform first principles calculations for ice Ih is currently limiting our choice as regards the computational methods available to us to density functional theory (DFT)[35] using a plane wave basis set. We will, nevertheless, assess the accuracy of this approach — both as regards the level of theory and the effect of the plane wave basis — from calculations on the clusters dimer through hexamer. The former is achieved by comparing the DFT results with the ones obtained using second order Møller–Plesset perturbation theory (MP2) with an atom-centered Gaussian basis set (common for the DFT and MP2 calculations). The latter effect associated with the adequacy of the plane wave basis is addressed by comparing the plane wave vs atom-centered basis set results within the same DFT scheme (i.e., using comparable functionals).

The DFT calculations with the plane wave basis set, carried out for water clusters up to the hexamer and ice Ih, were performed by explicitly including only the valence electrons;

the pseudopotentials of Troullier and Martins[36] were used. The wave functions were expanded in a plane wave basis set with an energy cutoff of 70 Rydberg (Ry). A total of 16 molecules were included in the ice Ih configuration. Only the Γ point (center) was used in the Brillouin zone sampling. As was shown by Lee et al.,[37] the local density approximation (LDA) gives a lattice constant for ice Ih that is 10% smaller than the experimental value while gradient dependent functionals resulted in a much better agreement with experiment. We have used the Perdew–Wang (PW91) gradient corrected functional[38] and obtained a nearest neighbor O–O separation of 2.7 Å at 0 K which is just 2% smaller than the experimental value. The PW91 functional used in the plane wave calculations contains both electron correlation and exchange terms. Both the cluster and ice configurations were relaxed until the magnitude of the force on each of the ions dropped below 0.1 eV/Å.

The ice Ih configuration was constructed in order to satisfy the ''ice-rules''[39] and the proton ordering was chosen to be anti-ferroelectric rather than random because of the small system size. In order to probe the electric field in a region that is relevant for intermolecular interactions, we removed one molecule from the ice configuration in order to create a vacancy. The configuration was then relaxed. The four molecules adjacent to the vacancy moved towards the vacancy site by 0.53, 0.51, 0.31, and 0.15 Å, respectively. The charge density was then used to calculate the total electric field at various points in the vacancy region.

Calculations of the multipole moments of an isolated water molecule and of the field near water clusters were also carried out using second order Møller–Plesset perturbation theory (MP2), analogous to previous MP2 calculations of water clusters.[40–44] The aug-cc-pVDZ basis set[45] was used in the MP2 and Gaussian-based DFT calculations. For the latter, we used the Becke exchange[46] and the PW91 correlation[38] functionals. All MP2 and DFT calculations with the Gaussian basis set were performed with the GAUSSIAN 94 suite of programs.[47]

The optimal structures for the clusters dimer through pentamer at the BPW91/aug-cc-pVDZ level are of similar quality to the ones previously reported with the same basis set and the BLYP functional.[42] Typical differences for the intermolecular coordinates from the MP2/aug-cc-pVDZ results[41,42] are <0.015 Å for the O···O distances and <2.0 degrees for the angles involved in the hydrogen bond. The cluster binding energies exhibit, however, larger deviations having values that are intermediate between HF and MP2 results.[42] As regards the effect of the plane wave basis set, the DFT results for the optimal geometries of the clusters exhibit the following absolute differences with respect to the ones with the MP2/aug-cc-pVDZ for the dimer through hexamer: (i) O–O distances: −0.053 Å, <−0.008 Å, −0.048 Å, <−0.015, Å and <−0.035 Å, (ii) hydrogen bond angles: 4, <1, <1.5, <2, and <0.2 degrees. Furthermore, the largest deviation in the dihedral angles is 7 degrees.

Finally, the MP2 multipole moments of an isolated water molecule were used in the induction model (see Sec. III and Table I). As it will be discussed later in this paper, the elec-

J. Chem. Phys., Vol. 112, No. 7, 15 February 2000

Electric fields in ice and near water clusters   3287

TABLE I. Multipole moments of a water molecule used in the induction model. The definition of the moments is given in the Appendix. The origin of the coordinate system is located at the center-of-mass of the molecule. The experimental value for the dipole moment is from Ref. 48 and the quadrupole moments are taken from Ref. 49.

		Exp	MP2	
Dipole	$\mathcal{P}_3$	−1.855	−1.86	$\times 10^{-18}$ e.s.u. cm
Quadrupole	$\mathcal{Q}_{33}$	−0.13	−0.1328	$\times 10^{-26}$ e.s.u. cm^2
	$\mathcal{Q}_{11}$	2.63	2.6135	
	$\mathcal{Q}_{22}$	−2.50	−2.4807	
Octopole	$\mathcal{O}_{333}$		1.3565	$\times 10^{-34}$ e.s.u. cm^3
	$\mathcal{O}_{113}$		−2.3288	
	$\mathcal{O}_{223}$		0.9723	
Hexadecapole	$\mathcal{H}_{3333}$		−1.3637	$\times 10^{-42}$ e.s.u. cm^4
	$\mathcal{H}_{1133}$		1.6324	
	$\mathcal{H}_{2233}$		−0.2687	
	$\mathcal{H}_{1111}$		−0.3575	
	$\mathcal{H}_{1122}$		−1.2749	
	$\mathcal{H}_{2222}$		1.5436	

tric field at the water clusters obtained from the MP2 was very similar to that obtained from the DFT calculations.

III. THE INDUCTION MODEL

The induction model uses information solely from an isolated water molecule. The polarizability of each molecule is taken into account by allowing the total field at a water molecule to induce dipole and quadrupole moments, thereby taking into account to some extent the environment of the molecule. The ith component of the induced dipole moment is given by[21]

$$\Delta \mathcal{P}_i = \alpha_{ij} E_j + \frac{1}{3} A_{i,jk} \frac{\partial E_j}{\partial r_k} + \frac{1}{2} \beta_{ijk} E_j E_k . \qquad (1)$$

Here, $\vec{E}$ is the total electric field, α_{ij} is the molecular dipole polarizability, $A_{i,jk}$ the dipole-quadrupole polarizability, and β_{ijk} the first hyperpolarizability. The repeated indices are to be summed over.

The electric field also induces a quadrupole moment on each molecule[21]

$$\Delta \mathcal{Q}_{ij} = A_{k,ij} E_k + C_{ij,kl} \frac{\partial E_k}{\partial r_l} , \qquad (2)$$

where $C_{ij,kl}$ is the quadrupole–quadrupole polarizability.

Equations (1) and (2) are implicit equations of $\mathcal{P}_i$ and $\mathcal{Q}_{ij}$. A given molecule polarizes its neighbors and these polarized neighbors are the ones that induce the additional dipole and quadrupole. We used an iterative procedure to solve these nonlinear equations.

A first order correction to the dipole moment of each molecule is induced by the total electric field of the neighboring unpolarized molecules

$$\Delta \mathcal{P}_i^{(1)} = \alpha_{ij} E_j^{(0)} + \frac{1}{3} A_{i,jk} \frac{\partial E_j^{(0)}}{\partial r_k} + \frac{1}{2} \beta_{ijk} E_j^{(0)} E_k^{(0)} , \qquad (3)$$

and, similarly, a first order correction to the quadrupole moment according to

$$\Delta \mathcal{Q}_{ij}^{(1)} = A_{k,ij} E_k^{(0)} + C_{ij,kl} \frac{\partial E_k^{(0)}}{\partial r_l} . \qquad (4)$$

The first order induced dipole moments create an additional electric field $\vec{E}_d^{(1)}$ and the induced quadrupole moments generate an additional electric field $\vec{E}_q^{(1)}$. The total first order correction field, $\vec{E}^{(1)} = \vec{E}_d^{(1)} + \vec{E}_q^{(1)}$ induces a second order correction to the dipole moment

$$\Delta \mathcal{P}_i^{(2)} = \alpha_{ij} E_j^{(1)} + \frac{1}{3} A_{i,jk} \frac{\partial E_j^{(1)}}{\partial r_k} + \frac{1}{2} \beta_{ijk} E_j^{(1)} E_k^{(1)} , \qquad (5)$$

and a second order correction to the quadrupole moment

$$\Delta \mathcal{Q}_{ij}^{(2)} = A_{k,ij} E_k^{(1)} + C_{ij,kl} \frac{\partial E_k^{(1)}}{\partial r_l} . \qquad (6)$$

The new induced multipoles in turn, create an additional electric field $\vec{E}^{(2)}$. This procedure continues until the magnitudes of the nth induced dipole,

$$\Delta \mathcal{P}_i^{(n)} = \alpha_{ij} E_j^{(n-1)} + \frac{1}{3} A_{i,jk} \frac{\partial E_j^{(n-1)}}{\partial r_k} + \frac{1}{2} \beta_{ijk} E_j^{(n-1)} E_k^{(n-1)} , \qquad (7)$$

and quadrupole moments

$$\Delta \mathcal{Q}_{ij}^{(n)} = A_{k,ij} E_k^{(n-1)} + C_{ij,kl} \frac{\partial E_k^{(n-1)}}{\partial r_l} , \qquad (8)$$

are smaller than a given tolerance. The iterative procedure was carried out until the corrections were smaller than 10^{-6} D and 10^{-6} D Å, respectively. Thus, self consistency was obtained up to this level of accuracy.

To calculate the electric field using the induction model, each molecule was represented with a point dipole, quadrupole, octopole, and a hexadecapole moment tensor at the center-of-mass. We used the experimentally measured dipole[48] and quadrupole moments [49] but the octopole and hexadecapole moments were obtained from MP2/aug-cc-pVQZ calculations. The values of the multipole moments are summarized in Table I. In addition to the multiple moments, the induction calculations made use of the experimentally measured molecular dipole polarizability, α_{ij},[50] and results of previous *ab initio* calculations for the values of the dipole–quadrupole, $A_{i,jk}$, and quadrupole–quadrupole polarizability, $C_{ij,kl}$[51] as well as the first hyperpolarizability, β_{ijk}.[52] The values of the polarizabilities are summarized in Table II. This induction model was previously used to estimate the multipole moments of water molecules in ice.[16]

At short range, the multipole expansion diverges. Following Millot *et al.*[53] we have used a switching function which reduces the field at short distances. The form of the switching function used here is the same as that used by Millot *et al.* but the decay length was chosen to be 4.4 Å, the exponential decay length of the charge density of the water molecule.

There is no *a priori* guarantee that the induction model will accurately predict the electric field in and around configurations of two or more water molecules. The molecular

TABLE II. Values of the polarizabilities used in the induction model. All quantities are in atomic units ($[\alpha_{ij}]=a_0^3$, $[\beta_{ijk}]=a_0^6/ea_0$, and $[A_{i,jk}]=a_0^4$). The coordinate reference frame of the molecule was defined as: $\hat{e}_1$ along the bisector of the molecule, axis $\hat{e}_2$ perpendicular to $\hat{e}_1$ and on the plane of the molecule, and axis $\hat{e}_3=\hat{e}_1\times\hat{e}_2$.

α_{11}	9.907 ± 0.02
α_{22}	10.311 ± 0.088
α_{33}	9.549 ± 0.088
$\alpha_{\text{isotropic}}$	9.922
β_{111}	5.4715
β_{122}	0.5445
β_{133}	10.029
$A_{1,11}$	-1.355
$A_{1,22}$	4.754
$A_{1,33}$	-3.399
$A_{2,12}$	-8.258
$A_{3,13}$	2.477

polarizability could, for example, change significantly in going from an isolated molecule to a water cluster and to ice. In the next section we describe tests of the induction model where the predicted electric field is compared to the one obtained from first principles calculations.

IV. RESULTS

The dominant attractive interaction between water molecules is believed to be the electrostatic interaction. To compare the induction model with the first principles calculations, we computed the total electric field at points located in a vacancy in the ice Ih lattice and around water clusters. On one hand, the electrostatic potential and electric field were calculated from the DFT charge density as

$$U(\mathbf{r})=\int_{\text{all space}}d^3r'\frac{\rho(\mathbf{r}')}{|\mathbf{r}-\mathbf{r}'|} \quad (9)$$

and,

$$\vec{E}(\mathbf{r})=\int_{\text{all space}}d^3r'\frac{\rho(\mathbf{r}')(\mathbf{r}-\mathbf{r}')}{|\mathbf{r}-\mathbf{r}'|^3}. \quad (10)$$

On the other hand we calculated the same quantities from the molecular multipole description of the system [see Eqs. (A6) and (A7) in the Appendix].

Figure 1 shows the magnitude of the electric field in a vacancy in an ice Ih crystal. The field predicted by the induction model reproduces quite well the electric field calculated directly from the first principles DFT charge density if the multipole expansion is carried out up to and including the hexadecapole. A total of 33 points were sampled inside the vacancy. The points were distributed along the line segments between the center of the vacancy towards the nearest molecules. The distance from each sampling point to the center of charge of the nearest molecule in the crystal is shown in Fig. 2. Note that the field due to only the molecular dipoles is significantly smaller than the total field. Adding the quadrupolar and octopolar contributions increases the field significantly and actually overshoots the total field by the time the octopole has been added. The hexadecapole contribution then reduces its magnitude and yields very good agreement with the total field. These calculations show that an induction model including up to hexadecapoles should give a good representation of the electrostatic interactions of water molecules for intermolecular separations typical for condensed phases.

Table III (last column) shows the convergence of the electric field as a function of the order of the multipole expansion. Each entry in the table is an average over the sampled points. The table gives the ratio of the multipolar field to the total field calculated from the DFT charge density. Even though the dipole field is the most important contributor to the total electric field, it is important to also include higher order multipoles, up to hexadecapole, because of the proximity to the neighboring water molecules.

The question naturally arises whether first principles calculations can be used to extract multipole moments that can be used in an induction model. The decomposition of the charge density into molecular fragments is, however, very arbitrary and many different decomposition methods have been proposed. We first used the atoms in molecules (AIM) method of Bader[28] where zero flux surfaces are used as di-
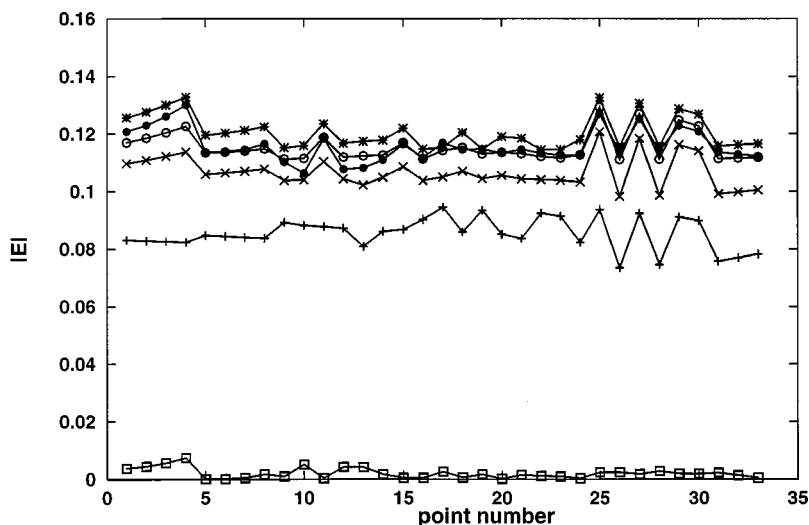

FIG. 1. Magnitude of the electric field inside a vacancy in ice Ih calculated using the DFT charge density (solid circles) and the induction model. While the dipolar field (+) of the induction model is the largest component, it only accounts for 70%–80% of the total field. For a better description of the electric field it is necessary to include quadrupole (×), octopole (*) and hexadecapole contributions (open circles). The open squares trace the difference between the DFT field and the multipolar field including up to hexadecapoles. The points are sorted by the distance to the nearest center of charge which is given in Fig. 2.
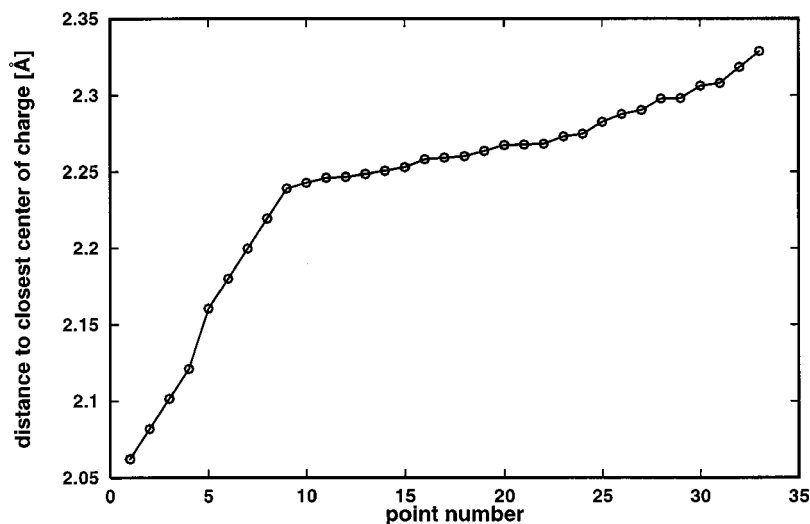
FIG. 2. Distance from the various points inside the vacancy in ice at which the electric field was sampled (see Figs. 1, 3, and 4) to the center of charge of the nearest water molecule in the relaxed ice lattice.

viding surfaces between the different molecules. The calculations were carried out using an elastic sheet method for finding the zero flux surfaces.[54] The resulting molecular dipole moments of water molecules in ice Ih are given in Table IV. The AIM scheme produces significantly smaller dipole moments than the induction model. The field inside a vacancy in ice calculated using the multipole moments of the AIM molecules is shown in Fig. 3 (see also Table III). While the dipole field is smaller than the dipole field in the induction model, convergence to the full field has nearly been reached when moments up to the hexadecapole are included. Significantly different values of the molecular multipoles can, therefore, be equally valid for practical purposes. To test how sensitive the first principles molecular moments are to the partitioning scheme, we also partitioned the calculated electron density using a Voronoi cell construction with a center placed at the center-of-mass of each molecule (Voronoi I scheme) as well as a Voronoi cell construction where a center is placed on each of the oxygen atoms and on each of the O–H bonds, 40% of the bond distance towards the H atoms (Voronoi II scheme). By including three centers the boundaries of the Voronoi cells can be made to lie near the region of minimal electron density between the molecules. While these two Voronoi schemes give significantly different values for the molecular dipole moment (see Table IV), the rate of convergence to the electric field obtained

from first principles is again quite similar, as can be seen in Fig. 4. The convergence of the Voronoi I scheme is, however, slightly slower.

The Voronoi II scheme which gives the smallest molecular dipole moment converges about as fast as the AIM scheme. The rate of convergence of the electric field using the various decomposition schemes for defining the molecular multipole moments is so similar that it is difficult to say that one is distinctly better than another.

The same conclusions are reached from studies of the electric field around small water clusters. Figure 5 shows the electric field evaluated on the surface of a sphere around the cyclic water trimer computed from the MP2 charge density (diamonds) and by summing up the various contributions using the induction model (solid line). About 1177 points were uniformly sampled on the surface of the sphere starting at the north pole and moving down in circles of increasing latitude towards the equator, which contains the three oxygen atoms. Only the field on the north hemisphere is shown (600 points). The zigzag pattern arises because the points are sampled on circles of increasing radius from zero to the radius of the sphere. Results for two values of the radius are

TABLE III. Ratio of the magnitude of the electric field in a vacancy in ice calculated using the multipole expansion and the magnitude of the field calculated from the DFT charge density. The convergence of the multipole expansion can be seen as more terms are added to the expansion: $\mathcal{P}$ stands for dipole, $\mathcal{Q}$ for quadrupole, $\mathcal{O}$ for octopole, and $\mathcal{H}$ for hexadecapole. The average over the various points inside the vacancy is given as well as the standard deviation.

	AIM	Voronoi I	Voronoi II	Induction
$\mathcal{P}$	0.73 ± 0.05	0.76 ± 0.06	0.66 ± 0.05	0.74 ± 0.05
$\mathcal{P}+\mathcal{Q}$	0.88 ± 0.03	0.94 ± 0.03	0.82 ± 0.02	0.92 ± 0.03
$\mathcal{P}+\mathcal{Q}+\mathcal{O}$	1.10 ± 0.03	1.17 ± 0.03	1.04 ± 0.02	1.04 ± 0.02
$\mathcal{P}+\mathcal{Q}+\mathcal{O}+\mathcal{H}$	1.03 ± 0.02	1.07 ± 0.03	0.96 ± 0.02	1.00 ± 0.02

TABLE IV. Average molecular dipole moment of a water molecule in ice Ih calculated by various methods. The induction model includes polarizable dipole and quadrupole as well as fixed octopole and hexadecapole and uses exclusively parameters from an isolated water molecule. The AIM method of Bader divides the electronic charge density with zero flux surfaces. The Voronoi I scheme involves constructing Voronoi cells around the center-of-mass of each molecule. In the Voronoi II scheme three Voronoi centers are used for each molecule, one placed at the oxygen atom, and the other two placed on the H–O bonds, 40% of the bondlength towards the H atom. The resulting values for the dipole moment are very different, but the multipole expansion of the electric field converges at a similar rate to the field obtained from the full electron density (see Figs. 1, 3, and 4 and Table III).

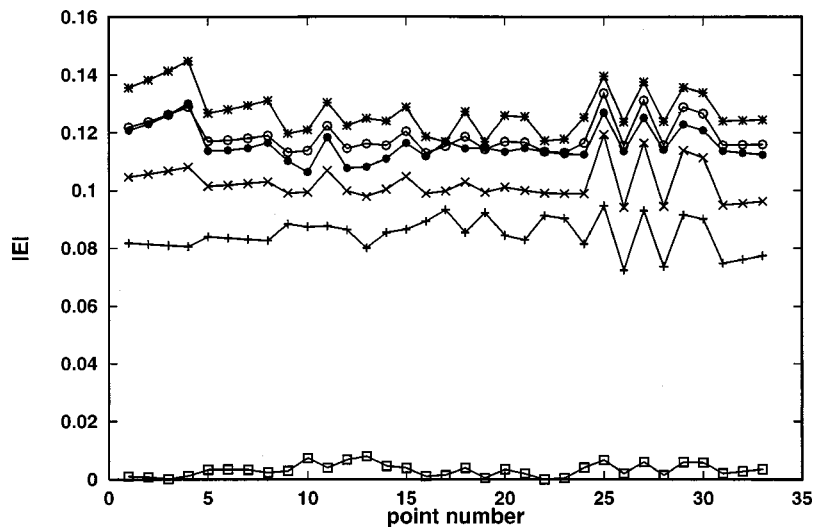| Method	$\mathcal{P}$ (Debye)
Induction	3.10
AIM	2.75
Voronoi I	2.97
Voronoi II	2.33

FIG. 3. Magnitude of the electric field inside a vacancy in ice Ih calculated using multipoles obtained from the AIM decomposition of the DFT charge density and from the DFT charge density directly (solid circles). While the dipolar field is significantly smaller using the AIM dipoles when compared to the induction model, the AIM multipole expansion converges at a similar rate as the induction model. Good agreement is obtained with the field deduced from the full DFT charge density when the expansion is carried out up to the hexadecapole. Various components of the AIM field are shown (the notation of the various components is the same as in Fig. 1).

shown, 4 and 5 Å. The oxygen atom of an additional fourth water molecule would be ~4.4 Å from the center of the sphere. The agreement is good and it gets better the further away from the cluster molecules the comparison is made. Closer to the center of the cluster, the electric charge density becomes significant. Since the multipole expansion of a charge density converges only when the field point is outside the charge distribution, the two calculations start to disagree significantly at shorter distances.

Figure 6 shows an analogous comparison for the cyclic hexamer water cluster. The electric field at a distance relevant for the binding of an additional water molecule is smaller in the case of the hexamer than the trimer because of cancellations. The agreement between the field evaluated from the induction model and the field calculated directly from the MP2 charge density is still good. Similar results were obtained for the tetramer and pentamer clusters.

V. DISCUSSION AND CONCLUSIONS

The success of the induction model, which only requires data that can be obtained from first principles calculations of the isolated water molecule, is very encouraging. This sug-

gests that an accurate description of the electrostatic interaction of water molecules can be achieved without having to carry out the computationally demanding first principles calculations for large systems. We are currently developing an empirical potential function based on the multipole expansion including the hexadecapole and both dipole and quadrupole polarizabilities. Interaction potentials for water molecules based on distributed multipole expansions have been previously introduced[24,25] but they are very costly to evaluate and thus have so far only been applied to small clusters. By including only multipoles with respect to the center-of-mass, as seems to be adequate from Figs. 1 and 5, the evaluation of the electric field can be done quite efficiently. Since no point charges are included, it is not necessary to use Ewald summation. In fact, it is sufficient to include only the field from neighbors within an 8 Å radius.[16] The multipole description of the electrostatic interactions is more accurate than the various point charge models which are frequently used in computer simulations of water. Since the Ewald sum can be avoided, the evaluation of the multipole expansion for ice surfaces does not involve significantly larger computational effort than the simple point charge models. The electric field
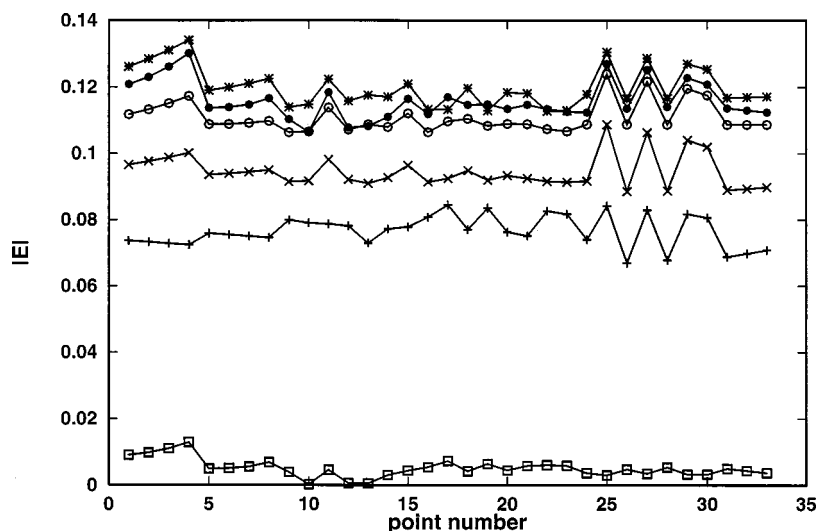

FIG. 4. Magnitude of the electric field inside a vacancy in ice Ih calculated using multipoles obtained from the Voronoi II decomposition of the DFT charge density and from the DFT charge density directly (solid circles). The Voronoi II multipole expansion converges at a similar rate as the induction model and the AIM multipole expansion, even though the molecular dipole moments are smaller. Good agreement is obtained with the field deduced from the full DFT charge density at the hexadecapole. Various components of the Voronoi II field are shown (the notation of the various components is the same as in Fig. 1).
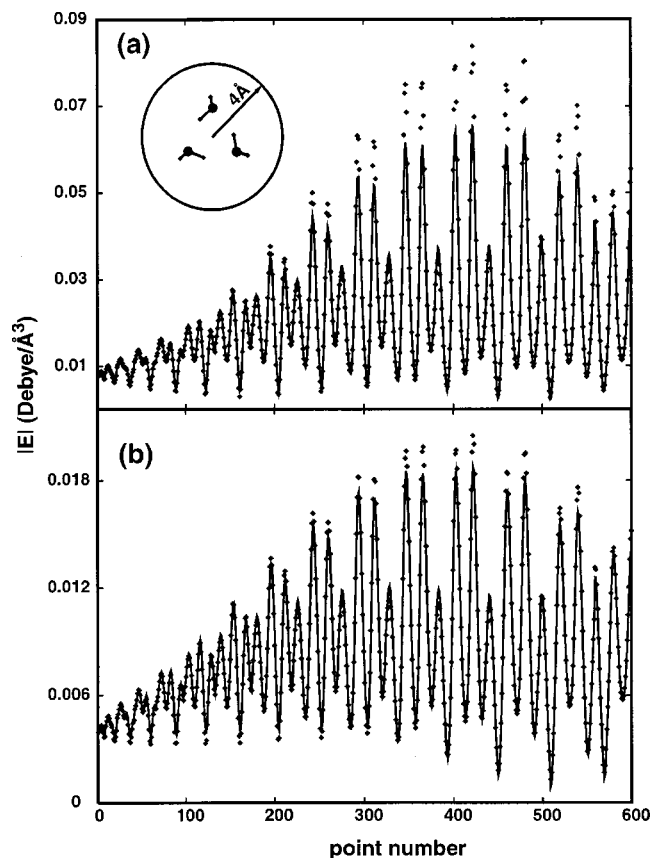
FIG. 5. Magnitude of the electric field around a water trimer calculated from the MP2 charge density (solid diamonds) and by using the induction model (solid line). The field was calculated at points located on a sphere centered at the center of the trimer. In (a) the radius of the sphere was 4 Å; in (b) the radius of the sphere is 5 Å. The field on the upper hemisphere is shown (the lower hemisphere gave similar results). The horizontal axis is the sample point number. 1177 points were sampled uniformly over the surface of the sphere starting at the upper pole and moving down to the equator which contains the three oxygen atoms.
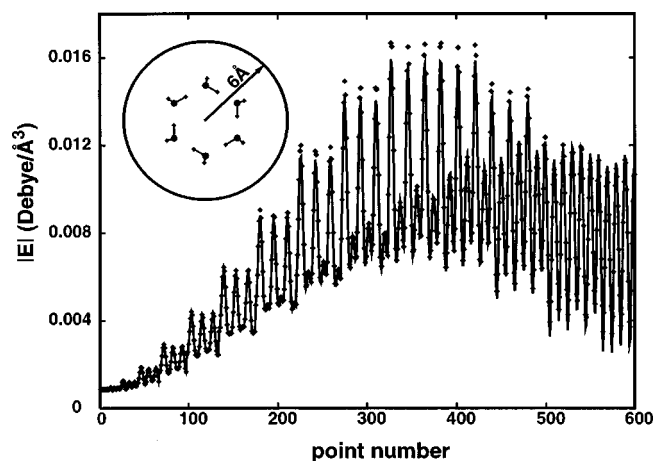

FIG. 6. Magnitude of the electric field around a water hexamer calculated from the MP2 charge density (solid diamonds) and by using the induction model (solid line). The field was calculated at points placed on the surface of a sphere centered at the center of the hexamer with a radius of 6 Å. The field on the upper hemisphere is shown (the lower hemisphere gave similar results). The horizontal axis is the sample point number. Points were sampled uniformly over the surface of the sphere starting at the upper pole and moving down to the equator.

generated by a typical point charge model does not agree well with the one obtained from first principles calculations. For example, the field calculated using the TIP4P point charge model,[55] an empirical potential which has been very successful in reproducing properties of bulk liquid water, gives an electric field that is about 20% larger than the one obtained from first principles in the ice vacancy. Our results suggest that an accurate interaction potential for water that is transferable to various environments, such as small clusters and ice surfaces, can be constructed using a single center multipole expansion with a computational effort that is quite similar to that of simple, nontransferable pair potentials.

Finally, the large range of values of the molecular dipole moments in ice obtained by using different reasonable schemes for extracting molecular dipole moments from first principles charge densities illustrates how poorly defined the molecular multipole moments are. The fact that the different schemes give very similar rate of convergence to the full electric field means that there is not a clear compelling reason to choose one over the other.

ACKNOWLEDGMENTS

APPENDIX: DEFINITIONS OF MULTIPOLE MOMENTS

Several different definitions of the multipole moments of a charge density are in use in the literature. The difference among them are signs, constants of proportionality and some being linear combinations of the others. In this appendix we give the definitions of the multipoles moments in Cartesian coordinates.

The total charge density of the molecule $\rho(\mathbf{r})$ is

$$\rho(\mathbf{r}) = \rho_e(\mathbf{r}) + \sum_i q_i \delta(\mathbf{r} - \mathbf{r}^{(i)}), \tag{A1}$$

where ρ_e is the electronic charge density, q_i and $\mathbf{r^{(i)}}$ are the ionic charge (one proton charge for each of the hydrogen atoms and eight for the oxygen) and the position of the ith ion, respectively, $\delta(\mathbf{r})$ is the Dirac delta function, and the sum is over all the nuclear charges. The molecular multipole moments are obtained by integrating over the charge density of the molecule. The electric dipole moment is defined as

$$\mathcal{P}_i = \int d^3 r \rho(\mathbf{r}) r_i. \tag{A2}$$

The quadrupole moment is defined as

$$\mathcal{Q}_{ij} = \frac{1}{2} \int d^3 r \rho(\mathbf{r}) (3 r_i r_j - r^2 \delta_{ij}), \tag{A3}$$

where δ_{ij} is the Kroneker delta. We chose to measure $\mathbf{r}$ from the center-of-mass of the molecule. The octopole moments are defined as

3292   J. Chem. Phys., Vol. 112, No. 7, 15 February 2000

Batista, Xantheas, and Jónsson

$$\mathcal{O}_{ijk} = \frac{1}{3!} \int d^3 r \rho(\mathbf{r}) [15 r_i r_j r_k - 3r^2 (r_i \delta_{jk} + r_j \delta_{ki} + r_k \delta_{ij})],$$
(A4)

and the components of the hexadecapole as

$$\mathcal{H}_{ijkl} = \frac{1}{4!} \int d^3 r \rho(\mathbf{r}) [105 r_i r_j r_k r_l - 15 r^2 (r_i r_j \delta_{kl} + r_i r_k \delta_{jl}$$
$$+ r_i r_l \delta_{jk} + r_j r_k \delta_{il} + r_j r_l \delta_{ik} + r_k r_l \delta_{ij})$$
$$+ 3r^4 (\delta_{ij} \delta_{kl} + \delta_{ik} \delta_{jl} + \delta_{il} \delta_{jk})].$$
(A5)

With these definitions, the electrostatic potential generated by a molecule is

$$U = \frac{\mathcal{P}_i r_i}{r^3} + \frac{\mathcal{Q}_{ij} r_i r_j}{r^5} + \frac{\mathcal{O}_{ijk} r_i r_j r_k}{r^7} + \frac{\mathcal{H}_{ijkl} r_i r_j r_k r_l}{r^9}.$$
(A6)

The electric field can be obtained from the gradient of Eq. (A6)

$$\vec{E}(\mathbf{r}) = \vec{E}_d(\mathbf{r}) + \vec{E}_q(\mathbf{r}) + \vec{E}_o(\vec{r}) + \vec{E}_h(\mathbf{r})$$
(A7)

where the dipole field is

$$E_d(\mathbf{r})_n = 3 \frac{\mathcal{P}_i r_i}{r^5} r_n - \frac{\mathcal{P}_n}{r^3},$$
(A8)

the quadrupole field is

$$E_q(\mathbf{r})_n = 5 \frac{\mathcal{Q}_{ij} r_i r_j}{r^7} r_n - 2 \frac{\mathcal{Q}_{in} r_i}{r^5},$$
(A9)

the octopole field is

$$E_o(\mathbf{r})_n = 7 \frac{\mathcal{O}_{ijk} r_i r_j r_k}{r^9} r_n - 3 \frac{\mathcal{O}_{nij} r_i r_j}{r^7},$$
(A10)

and the hexadecapole field is

$$E_h(\mathbf{r})_n = 9 \frac{\mathcal{H}_{ijkl} r_i r_j r_k r_l}{r^{11}} r_n - 4 \frac{\mathcal{H}_{nijk} r_i r_j r_k}{r^9}.$$
(A11)

[1] T. P. Lybrand and P. A. Kollman, J. Chem. Phys. **83**, 2923 (1985).

[2] J. Caldwell, L. X. Dang, and P. A. Kollman, J. Am. Chem. Soc. **112**, 9145 (1990).

[3] L. X. Dang and T.-M. Chang, J. Chem. Phys. **106**, 8149 (1997).

[4] C. J. Burnham, J. Li, S. S. Xantheas, and M. Leslie, J. Chem. Phys. **110**, 4566 (1999).

[5] C. Coulson and D. Eisenberg, Proc. R. Soc. London, Ser. A **291**, 445 (1966).

[6] E. Whalley, J. Glaciol. **21**, 13 (1978).

[7] D. Adams, Nature (London) **293**, 447 (1981).

[8] M. Sprik, J. Chem. Phys. **95**, 6762 (1991).

[9] K. Laasonen, M. Sprik, M. Parrinello, and R. Car, J. Chem. Phys. **99**, 9080 (1993).

[10] D. Wei and D. R. Salahub, Chem. Phys. Lett. **224**, 291 (1994).

[11] E. S. Fois, M. Sprik, and M. Parrinello, Chem. Phys. Lett. **223**, 411 (1994).

[12] C. Gatti, B. Silvi, and F. Colonna, Chem. Phys. Lett. **247**, 135 (1995).

[13] M. I. Heggie, C. D. Latham, S. C. P. Maynard, and R. Jones, Chem. Phys. Lett. **249**, 485 (1996).

[14] J. K. Gregory, D. C. Clary, K. Liu, M. G. Brown, and R. J. Saykally, Science **275**, 814 (1997).

[15] K. Liu, M. G. Brown, and R. J. Saykally, J. Phys. Chem. A **101**, 8995 (1997).

[16] E. R. Batista, S. S. Xantheas, and H. Jónsson, J. Chem. Phys. **109**, 4546 (1998).

[17] P. L. Silvestrelli and M. Parrinello, Phys. Rev. Lett. **82**, 3308 (1999).

[18] L. Delle Site, A. Alavi, and R. M. Lynden-Bell, Mol. Phys. **96**, 1683 (1999).

[19] P. Barnes, J. L. Finney, J. D. Nicholas, and J. E. Quinn, Nature (London) **282**, 459 (1979).

[20] A. D. Buckingham, Adv. Chem. Phys. **12**, 107 (1967).

[21] A. J. Stone, *The Theory of Intermolecular Forces* (Clarendon, Oxford, 1996).

[22] R. S. Mulliken, J. Chem. Phys. **23**, 1833 (1955).

[23] C. Edmiston and K. Ruedenberg, Rev. Mod. Phys. **35**, 457 (1963).

[24] A. J. Stone, Chem. Phys. Lett. **83**, 233 (1981).

[25] A. J. Stone and M. Alderton, Mol. Phys. **56**, 1047 (1985).

[26] J. E. Carpenter and F. Weinhold, J. Mol. Struct.: THEOCHEM **169**, 41 (1988), and references therein.

[27] J. Pipek and P. G. Mezey, J. Chem. Phys. **90**, 4916 (1989).

[28] R. Bader, *Atoms in Molecules. A Quantum Theory* (Oxford University Press, Oxford, 1990).

[29] E. R. Batista, S. S. Xantheas, and H. Jónsson, J. Chem. Phys. **111**, 6011 (1999).

[30] C. E. Dykstra, J. Phys. Chem. **91**, 6216 (1987).

[31] J. Perez and M. Dupuis, J. Phys. Chem. **95**, 6526 (1991).

[32] S.-Y. Liu and C. E. Dykstra, J. Phys. Chem. **90**, 3097 (1986).

[33] D. J. Malik and C. E. Dykstra, J. Chem. Phys. **83**, 6307 (1985).

[34] J. D. Augsburger and C. E. Dykstra, J. Chem. Phys. **88**, 3817 (1988).

[35] P. Hohenberg and W. Kohn, Phys. Rev. **136**, 864 (1964); W. Kohn and L. J. Sham, Phys. Rev. **140**, 1133 (1965).

[36] N. Troullier and J. Martins, Phys. Rev. B **43**, 1993 (1991).

[37] C. Lee, D. Vanderbilt, K. Laasonen, R. Car, and M. Parrinello, Phys. Rev. B **47**, 4863 (1993).

[38] J. P. Perdew, in *Electronic Structure of Solids '91*, edited by P. Ziesche and H. Eschrig (Akamemie Verlag, Berlin, 1991), p. 11.

[39] J. D. Bernal and R. H. Fowler, J. Phys. Chem. **1**, 515 (1933).

[40] S. S. Xantheas and T. H. Dunning, Jr., J. Chem. Phys. **98**, 8037 (1993).

[41] S. S. Xantheas and T. H. Dunning, Jr., J. Chem. Phys. **99**, 8774 (1993).

[42] S. S. Xantheas, J. Chem. Phys. **102**, 4505 (1995).

[43] S. S. Xantheas, Philos. Mag. B **73**, 107 (1996).

[44] S. S. Xantheas and T. H. Dunning, Jr., in *Advances in Molecular Vibrations and Collision Dynamics*, edited by Z. Bacic and J. M. Bowman (JAI, 1998), Vol. 3, pp. 281–309.

[45] R. A. Kendall and T. H. Dunning, Jr., and R. J. Harrison, J. Chem. Phys. **96**, 6796 (1992).

[46] A. D. Becke, Phys. Rev. A **38**, 3098 (1988).

[47] GAUSSIAN 94, Revision **E.2**, M. J. Frisch, G. W. Trucks, H. B. Schlegel, P. M. W. Gill, B. G. Johnson, M. A. Robb, J. R. Cheeseman, T. Keith, G. A. Petersson, J. A. Montgomery, K. Raghavachari, M. A. Al-Laham, V. G. Zakrzewski, J. V. Ortiz, J. B. Foresman, J. Cioslowski, B. B. Stefanov, A. Nanayakkara, M. Challacombe, C. Y. Peng, P. Y. Ayala, W. Chen, M. W. Wong, J. L. Andres, E. S. Replogle, R. Gomperts, R. L. Martin, D. J. Fox, J. S. Binkley, D. J. Defrees, J. Baker, J. P. Stewart, M. Head-Gordon, C. Gonzalez, and J. A. Pople, *Gaussian, Inc.*, Pittsburgh PA, 1995.

[48] T. Dyke and J. Muenter, J. Chem. Phys. **59**, 3125 (1973).

[49] J. Verhoeven and A. Dymanus, J. Chem. Phys. **52**, 3222 (1970).

[50] W. F. Murphy, J. Chem. Phys. **67**, 5877 (1977).

[51] C. Millot and A. J. Stone, Mol. Phys. **77**, 439 (1992).

[52] C. E. Dykstra, S.-Y. Liu, and D. J. Malik, Adv. Chem. Phys. **75**, 37 (1989).

[53] C. Millot, J.-C. Soetens, M. T. C. Martins Costa, M. P. Hodges, and A. J. Stone, J. Chem. Phys. **102**, 754 (1998).

[54] B. P. Uberuaga, E. R. Batista, and H. Jónsson, J. Chem. Phys. **111**, 10664 (1999).

[55] W. L. Jorgensen, J. Chandrasekhar, J. D. Madura, R. W. Impey, and M. L. Klein, J. Chem. Phys. **79**, 926 (1983).